

# Computation of vortex-induced vibrations of long structures using a wake oscillator model: Comparison with DNS and experiments

R. Violette <sup>a,b</sup>, E. de Langre <sup>a,\*</sup>, J. Szydlowski <sup>b</sup>

<sup>a</sup> *Département de Mécanique, LadHyX, CNRS – Ecole Polytechnique, 91128 Palaiseau, France*

<sup>b</sup> *Institut Français du Pétrole, 1-4 av. de Bois Préau, 92852 Reuil-Malmaison, France*

Received 31 May 2006; accepted 22 August 2006

Available online 2 January 2007

## Abstract

We consider here the dynamics of flexible slender systems undergoing vortex-induced vibration (VIV). This type of motion results from the coupling between the oscillating wake due to cross-flow and the structure motion. Practical applications are mainly found in the field of ocean engineering, where long flexible structures such as risers or mooring cables are excited by sea currents. The wake dynamics is here represented using a distributed wake oscillator coupled to the dynamics of the slender structure, a cable or a tensioned beam. This results in two coupled partial differential equations with one variable for the solid displacement and one for the wake fluctuating lift. This simplified model of the wake dynamics has been previously validated on simple experiments. Here, comparisons with direct numerical simulation results are done for both uniform and non-uniform flow. Comparison is also performed between the wake oscillator predictions and some experimental results on long cables. The results of those comparisons show that the proposed method can be used as simple computational tool in the prediction of some aspects of vortex induced vibrations of long flexible structures.

© 2006 Elsevier Ltd. All rights reserved.

*Keywords:* Vortex-induced vibration; Wake oscillator; Cable; Van der Pol; Waves; Fluid–structure interaction

## 1. Introduction

Flow past a circular bluff body creates an unstable wake in the form of alternating vortices. Those vortices are shed from the cylinder at a frequency defined by the Strouhal law. They create periodically varying lift forces on the cylinder. The later, if flexible enough, undergoes vortex-induced vibration (VIV), see recent reviews by Williamson and Govardhan [21], Sarpkaya [18] and Gabbai and Benaroya [9]. Vortex-induced vibration is a major concern regarding fatigue life of marine structures like risers used in offshore petroleum production. The prediction of those VIV is still an open research field especially for risers of very large aspect ratio ( $L/D \sim 2000\text{--}3000$ ) subjected to depth varying flow. Since the vortex shedding frequency varies with flow velocity, a depth varying flow past a flex-

ible cylinder will result in multifrequency excitation. Depending on the range of velocity covered by the flow profile, many vibration modes of the structure can be excited. Understanding the vibration mechanisms of the structure in those cases is not a simple task. For instance, Vandiver [19] and Vandiver et al. [20] did experimental parametric studies of risers subjected to non-uniform flow in order to determine when the response is monomodal or multimodal. Marcollo and Hindwood [13] experimentally studied the mode competition of a flexible beam subjected to a step current. Recent experimental and numerical investigations such as in [5] and [1] showed the complexity of the issue of VIV of long flexible cylinders.

Numerous methods for predicting the dynamic behavior of structures experiencing vortex-induced vibration are available in the literature. One VIV prediction method consists of solving the Navier–Stokes equations by direct numerical simulation (DNS) for the fluid around the flexible cylinder and to compute the hydrodynamic loads

\* Corresponding author.

*E-mail address:* [delangre@ladhyx.polytechnique.fr](mailto:delangre@ladhyx.polytechnique.fr) (E. de Langre).

resulting on it. The deformation of the flexible cylinder and its resulting effect on the flow field is also computed, the two being coupled, see for instance [15]. An alternative approach is to model the principal features of vortex shedding in the cylinder wake using a dynamical system. The main difference between this phenomenological approach and DNS is that the dynamic behavior of the fluid in the cylinder wake is modeled instead of being computed. Bishop and Hassan [3] and Birkoff and Zarantanello [2] were the first to consider the use of the van der Pol oscillator equation to model the behavior of the cylinder wake. Hartlen and Curie [10] applied this concept and developed the first so called wake oscillator model that used the van der Pol oscillator equation for the cylinder wake modeling. Recently, the van der Pol oscillator was revisited for VIV prediction: Facchinetti et al. [7] verified the effect of the cylinder movement on the lift fluctuation via different type of coupling (displacement, velocity and acceleration). They came up with a formulation of the wake oscillator model that was qualitatively and, in some point, quantitatively reproducing some aspects of VIV observed experimentally for rigid cylinders elastically supported. Facchinetti et al. [8] extended the model to predict VIV and VIW (vortex-induced waves) for cables and successfully predicted the experimental response behavior of a towed cable. Mathelin and de Langre [14] pushed further Facchinetti's work to predict VIV of cables subjected to sheared flows.

The purpose of this paper is to verify, following [7,8,14], how this simple approach can predict some of the dynamics of cables or flexible beams observed in both DNS and experiments. Here, the focus is on cases of long flexible structures subjected to uniform and non-uniform flow. In

Section two of this paper, the VIV prediction model developed by Facchinetti et al. [8] and by Mathelin and de Langre [14] is summarized. In Section three, comparison of the wake oscillator model results is made with DNS results available in the literature for tensioned cables and beams subjected to uniform and non-uniform flow. The fourth section contains a comparison between the model and experimentally observed cable behavior.

## 2. Model description

The main features of the wake oscillator model by Facchinetti et al. [7], Facchinetti et al. [8] and by Mathelin and de Langre [14] are summarized in this section. A straight slender cylinder oscillating in the direction transverse to the flow is considered here (Fig. 1). The reference length scale used is the cylinder diameter  $D$ . The dimensional displacement  $Y$  and span position  $Z$  are  $Y = yD$  and  $Z = zD$ , respectively. The cylinder diameter, the Strouhal number  $St$  and an arbitrary reference flow velocity  $U_{ref}$  define the Strouhal pulsation of vortex shedding  $\Omega_{ref} = 2\pi St U_{ref}/D$ . This pulsation is used to define the reference time scale. The dimensional time  $T$  is thus expressed as  $T = t/\Omega_{ref}$ .

Considering the reference length and time scale mentioned above, the dynamics of a straight cylinder can be described by the dimensionless equation

$$\frac{\partial^2 y}{\partial t^2} - c^2 \frac{\partial^2 y}{\partial z^2} + b^2 \frac{\partial^4 y}{\partial z^4} = S - \frac{\gamma \omega_f}{\mu} \frac{\partial y}{\partial t}, \quad (1)$$

where  $y(z, t)$  is the lateral displacement (Fig. 1a). The dimensionless tension  $c$  is given by  $c^2 = (K/(m_{cyl} + m_{fluid})) / (\Omega_{ref} D)^2$

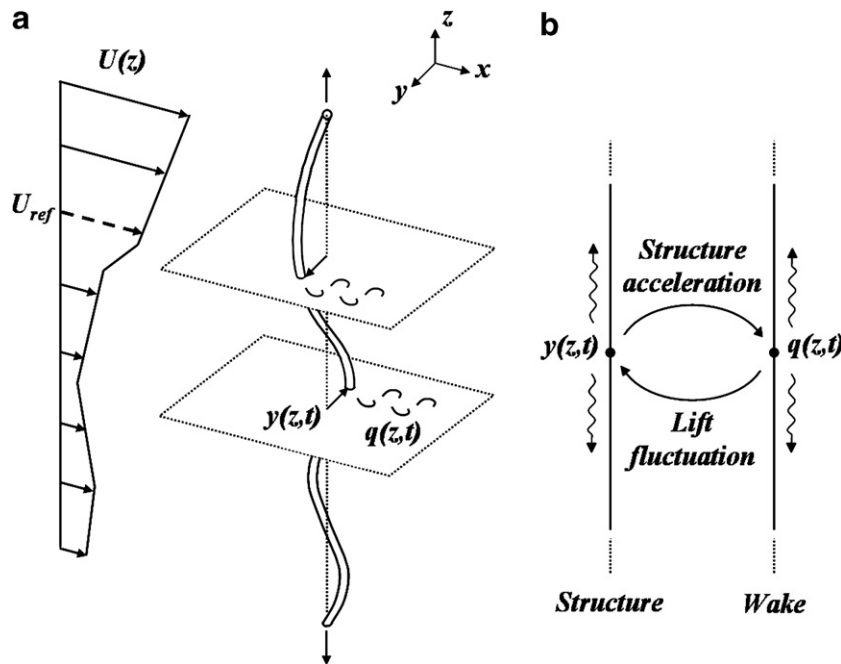


Fig. 1. Long flexible structure under a depth-varying flow: (a) definition of parameters and (b) present model using a distributed wake oscillator locally coupled with a tensioned beam, Eqs. (5) and (6).

and the dimensionless bending stiffness  $b$  by  $b^2 = (EI/(m_{\text{cyl}} + m_{\text{fluid}}))/(\Omega_{\text{ref}}^2 D^4)$ . The dimensional cylinder tension and bending stiffness are  $K$  and  $EI$ , respectively. The parameters  $m_{\text{cyl}}$  and  $m_{\text{fluid}}$  are the mass per unit length of the cylinder and the fluid added mass respectively. The second term on the right hand side of (1) is the fluid induced damping resulting from drag effects [4]. It depends on the mass ratio  $\mu = (m_{\text{cyl}} + m_{\text{fluid}})/\rho D^2$  where  $\rho$  is the fluid density, the normalized shedding pulsation  $\omega_f = \Omega(z)/\Omega_{\text{ref}} = U(z)/U_{\text{ref}}$  and the stall coefficient  $\gamma$ . The later is expressed as  $\gamma = C_D/4\pi St$  where  $C_D$  is the mean sectional drag coefficient. The fluid forcing term generated by the cylinder's wake,  $S$ , will be discussed below. The cylinder structural damping is neglected in this paper.

A forced van der Pol oscillator equation is used to describe the dynamics of the cylinder's wake

$$\frac{\partial^2 q}{\partial t^2} + \varepsilon \omega_f (q^2 - 1) \frac{\partial q}{\partial t} + \omega_f^2 q = G. \quad (2)$$

As in [7], the variable  $q$  is here defined as the local fluctuating lift coefficient  $q(z, t) = 2C_L(z, t)/C_{L0}$ , the coefficient  $C_{L0}$  is the amplitude of the fluctuating lift for a fixed rigid cylinder subjected to vortex shedding. The term  $G$  expresses the effect of the structure motion on the wake and is discussed below. In Eq. (2), the linear negative damping term allows for an amplitude increase of  $q$  if perturbed from  $q = 0$ . The non-linear term ensures the saturation of  $q$  for the unforced case ( $G = 0$ ). Note that all direct coupling of the wake variables in the  $z$ -direction is here neglected: a diffusion coupling was analysed in [6] but it was showed in [14] that it plays a negligible role when the cylinder motion is significant, as will be the case here.

The forcing term on the structure due to the wake dynamics in Eq. (1) is assumed to be

$$S = M \omega_f^2 q, \quad M = \frac{C_{L0}}{2} \frac{1}{8\pi^2 St^2 \mu}. \quad (3)$$

The forcing on the wake due to the cylinder motion in Eq. (2) has been evaluated by Facchinetti et al. [7], using experimental data of VIV of elementary systems (one degree of freedom) in uniform flow. They found that with the acceleration of the structure as the forcing term, the van der Pol model was qualitatively and, in some point, quantitatively describing some of the typical physics of vortex-induced vibrations observed experimentally. That way, the coupling term in Eq. (2) is expressed as

$$G = A \frac{\partial^2 y}{\partial t^2}. \quad (4)$$

The value of  $A$  in Eq. (4) as well as that of  $\varepsilon$  in Eq. (2) has been determined from experimental data of fluctuating lift on a rigid cylinder driven in forced vibration. The values found for those parameters are  $A = 12$  and  $\varepsilon = 0.3$  [7].

The set of partial differential equations in  $y(z, t)$  and  $q(z, t)$  to solve can be summarized as

$$\frac{\partial^2 y}{\partial t^2} + \frac{\gamma \omega_f}{\mu} \frac{\partial y}{\partial t} - c^2 \frac{\partial^2 y}{\partial z^2} + b^2 \frac{\partial^4 y}{\partial z^4} = \omega_f^2 M q \quad (5)$$

$$\frac{\partial^2 q}{\partial t^2} + \varepsilon \omega_f (q^2 - 1) \frac{\partial q}{\partial t} + \omega_f^2 q = A \frac{\partial^2 y}{\partial t^2}. \quad (6)$$

In this system, all coefficients can be estimated using particular characteristics of the flexible cylinder,  $D$ ,  $K$ ,  $EI$ ,  $m_{\text{cyl}}$ , of the flow,  $m_{\text{fluid}}$ ,  $\rho$ ,  $U(z)$ , and phenomenological parameters derived from elementary experiments on wake dynamics and vortex-induced vibrations. Those phenomenological parameters are  $St$ ,  $C_D$ ,  $C_{L0}$ ,  $A$  and  $\varepsilon$ . The Strouhal number  $St$ , drag coefficient  $C_D$  and fluctuating lift coefficient  $C_{L0}$  may for instance be found in [16] as they are only related to wake dynamics of fixed cylinders. The values of those parameters used throughout this paper are  $C_D = 1.2$ ,  $C_{L0} = 0.3$  and  $St = 0.2$  (except in Case I and II where  $St = 0.16$  for consistency with the reference data). All dimensionless coefficients in (5,6) are constant in the  $z$ -direction, except  $\omega_f(z)$  which depends on the local flow velocity  $U(z)$ . The dependence of phenomenological parameters with the Reynolds number, and therefore with  $z$  for non-uniform flows, is neglected here for the sake of clarity. This system is numerically integrated in time and space using a standard centered finite difference method of the second order in both domains. Description of this method can be found, for example, in [17]. The time step used in all calculation is chosen much smaller than the critical time step and its effect on the results was checked. Boundary conditions and initial conditions are described below for each case of computations.

### 3. Comparison with DNS results

The objective of this section is to verify if some aspect of the dynamics observed with DNS models predictions can be reproduced by the wake oscillator model described in the previous section. Fig. 2 shows a schematic representation of the three configurations analysed here.

The first case analysed is a simple tensioned cable subjected to uniform flow. Complexity is added in the following cases: in the second one, the flow is varying in a sinusoidal manner in space and in the third case, comparison is performed for a tensioned beam subjected to a linearly sheared flow.

#### 3.1. Case I: Infinite tensioned cable under uniform flow

Newman and Karniadakis [15] performed spectral DNS simulation studies of flexible cables under VIV conditions. They considered in particular the preferred response behavior of infinite cables subjected to a uniform flow. In order to limit the spatial computation domain, they imposed periodic conditions on the limits in  $z$ -direction. The geometrical changes of the computational domain due to the cylinder motion were taken into account by using body-fitted coordinates. They modeled the cylinder as a tensioned cable without structural damping. For the

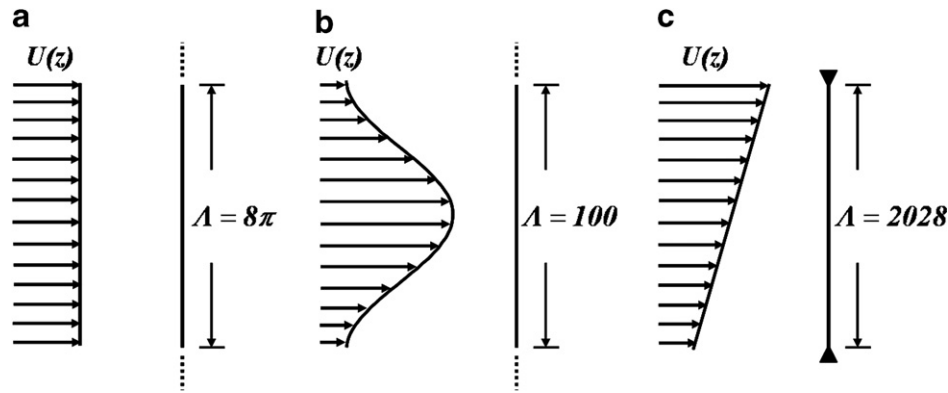


Fig. 2. Configurations used for comparison between predictions of DNS and wake oscillator model: (a) infinite tensioned cable under uniform flow, Case I; (b) infinite tensioned cable under non-uniform flow, Case II; (c) finite tensioned beam under linearly sheared flow, Case III;  $A$  is the aspect ratio  $L/D$ .

case considered in this section, Fig. 19(c) in Newman and Karniadakis [15], they used quasi-random initial conditions for the cable and the fluid variables.

The PDE system (5,6) is integrated for this particular cable configuration, extending the results of [8]. The parameters used in the simulation appear in Table 1 (Case I). Boundary conditions are posed as periodic on  $y$ :  $y(0, t) = y(A, t)$ . As initial conditions, a random noise with amplitude of order  $O(10^{-3})$  is applied to the fluid variable  $q$ . Zero displacement and velocity initial conditions are applied to the structure. The first time derivative of the fluid variable is also set to zero as initial condition. For the spatial discretization, 252 points are used for the simulation and a dimensionless time step of 0.01 is used. The integration is carried for a dimensionless time  $t$  of 600. The results obtained for DNS at a Reynolds number ( $U_{ref}D/\nu$ ) of 100 and wake oscillator model prediction appear in Fig. 3.

Fig. 3 shows the time evolution of the cable’s transverse displacement at every span position computed by the DNS (Fig. 3a) and wake oscillator model (Fig. 3b). One can observe that the frequency and wavelength are similar for

the two models. This is expected since in both cases the cable is tuned to resonate with the vortex shedding frequency at that particular mode. In the DNS results, a standing wave response for the cable emerges first. This standing wave progressively transforms into a travelling wave after several vibration cycles, typically 10. Fig. 3b clearly shows that this global behavior is well reproduced by the wake oscillator model. It also shows that the number of cycles for which the standing wave persists is quite comparable for both models. For the wake oscillator model, it is found that the travelling wave response constitutes the permanent vibration regime. The propagation direction of those travelling waves is arbitrary.

### 3.2. Case II: Infinite tensioned cable under non-uniform flow

In addition to the cases simulated for cables under uniform flow, Newman and Karniadakis [15] performed a computation for a tensioned cable under non uniform flow. The configuration they studied appears in Fig. 2b. (Fig. 26 in their paper). The flow profile is sinusoidal and the maximum flow velocity  $U_{max}$  is twice the minimum value  $U_{min}$ .

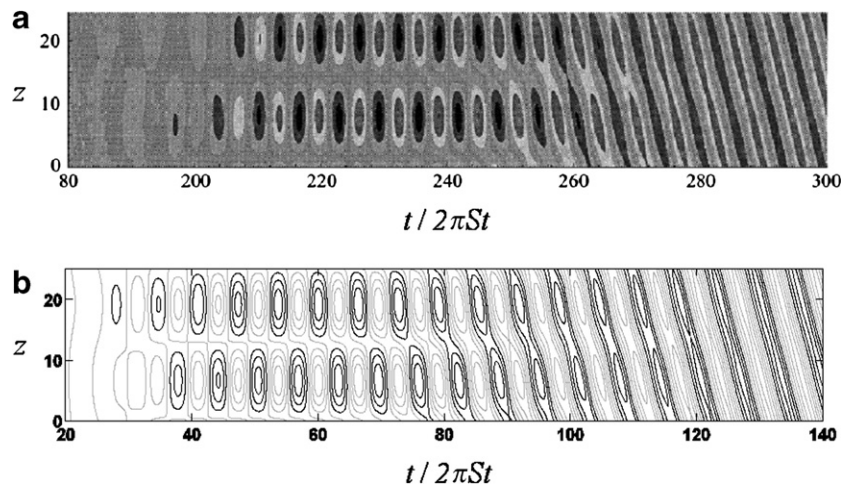


Fig. 3. Infinite tensioned cable under uniform flow, Case I. Evolution of cable displacement with time and space: (a) DNS [15] and (b) wake oscillator model. In both figures the displacement level is shown ranging from  $-0.6$  to  $0.6$  with equally spaced intervals.

The spatial computational domain is extended so that the aspect ratio now is  $A = 100$ . The Reynolds number corresponding to the maximum velocity is 100. The boundary conditions used are the same as for Case I. This case is now computed using the wake oscillator model. The parameters used in the simulation appear in Table 1. As initial conditions, zero displacement and velocity are imposed for the cable. A sinusoidal shape identical to the flow profile is used as initial value for the fluid variable  $q$ , with a magnitude of order  $O(10^{-3})$ . This particular choice of the initial value is discussed below. The time derivative of the fluid variable is set to zero as initial condition. The number of points used for the spatial integration is 1001 and a dimensionless time step of 0.01 is used for the integration. The PDE system is numerically integrated for a dimensionless time  $t$  of 800. The lowest flow velocity is used as reference  $U_{\text{ref}} = U_{\text{min}}$ . The results for both the DNS and the wake oscillator appear in Fig. 4a and b, respectively.

Fig. 4a shows that DNS predicts a combination of standing and travelling waves for the cable response. Standing waves dominate the response near the center and at the limits of the spatial computational domain. In between those regions, travelling waves can be observed. The wake oscillator (Fig. 4b) predicts the same dynamical behavior. Moreover, the prediction of wavelength, pulsation and wave velocity is similar for both computational methods. Note that in both DNS and wake oscillator simulations, the amplitude is the lowest at the center cable where the flow velocity is maximum, which is rather counter-intuitive.

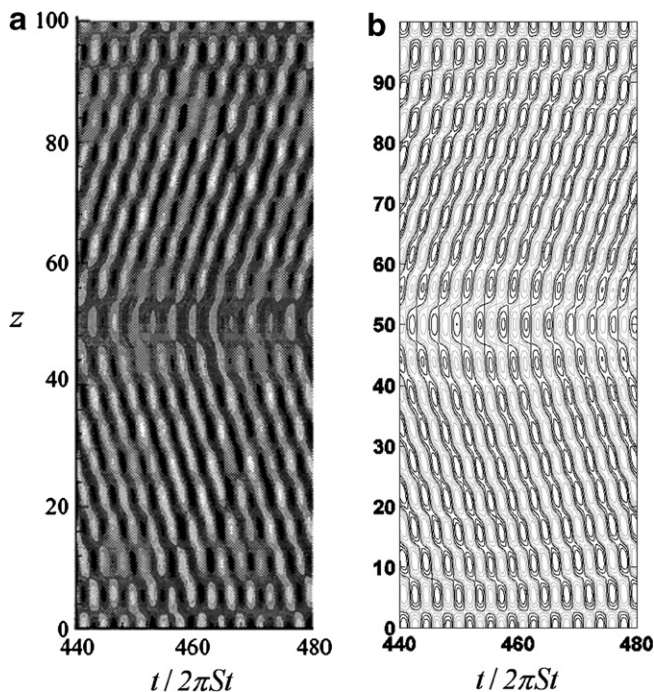


Fig. 4. Infinite tensioned cable under non-uniform flow, Case II. Evolution of cable displacement with time and space: (a) DNS [15] and (b) wake oscillator model. In both figures the displacement level is shown ranging from  $-0.4$  to  $0.4$  with equally spaced intervals.

Numerical simulations with the wake oscillator model were also done with a random noise of order  $O(10^{-3})$  amplitude as initial conditions for the fluid variable  $q$ . A different cable dynamical behavior was obtained: a combination of standing and travelling waves as the one shown in both Fig. 4a and b emerges first, but this regime is unstable and transforms into travelling waves response with a spatial modulation of the vibration amplitude. The cable response is thus found quite sensible to initial conditions. This instability of the regime shown in Fig. 4 is also found for sinusoidal initial conditions, but at a longer a time.

### 3.3. Case III: Finite tensioned beam under linearly shear flow

Lucor et al. [12] performed DNS simulations of a very high aspect ratio tensioned beam ( $A = 2028$ ) with non-uniform flow loading (Fig. 2c). They simulated a linearly sheared flow with a velocity variation of 70% of the maximum value ( $\Delta U/U_{\text{max}} = 0.7$ ). They used the tensioned beam equation with zero structural damping to model the structure. The Reynolds number for the simulation, based on the maximum flow velocity  $U_{\text{max}}$ , was 1000. The number of beam vibration modes included in the flow excitation frequency bandwidth is 14. The beam is pinned at both ends.

The same case is computed with the wake oscillator model. The parameters used for this calculation are shown in Table 1. For this case, 2000 points are used for the spatial discretization with a dimensionless time step of 0.001. The integration is carried for a dimensionless time  $t$  of 1600. A zero displacement and bending moment conditions are imposed on the boundaries for the beam. As for the case of a uniform flow shown earlier, a random noise of order  $O(10^{-3})$  amplitude is applied on the fluid variable  $q$  as initial conditions. The first time derivative of the fluid variable is set to zero at  $t = 0$ . Zero displacement and velocity are posed for the cable at  $t = 0$ . As in Lucor et al. [12], the maximum flow velocity is used as reference. The r.m.s. value of the transverse displacement obtained as a function of  $z$  is shown in Fig. 5a and b for the DNS and the wake oscillator model, respectively.

It can be concluded by comparing Fig. 5a and b that the DNS and the wake oscillator predictions display good similitude. The wake oscillator is able to model the pseudo standing waves near the beam's end predicted by the DNS model. Away from the beam ends, the DNS predicts that the travelling waves dominate the beam response. This is also predicted by the wake oscillator model.

Table 1  
Simulation parameters used in the wake oscillator model

	Case I	Case II	Case III	Case IV
$St$	0.16	0.16	0.2	0.2
$A$	$8\pi$	100	2028	781
$\mu$	1.785	1.785	2.785	1.75
$c$	4	3	23.6	33.1–47.1
$b$	0	0	303	0

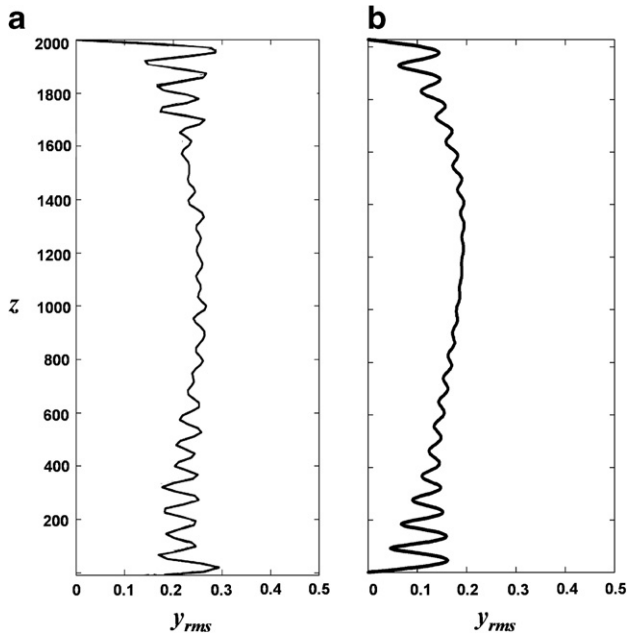


Fig. 5. Finite tensioned beam under linearly sheared flow, Case III. r.m.s. value of the displacement along the beam: (a) DNS [12] and (b) wake oscillator model.

#### 4. Comparison with experimental results

The ability of the wake oscillator to reproduce some predictions from DNS models has been addressed in the previous section. Here, the focus is on evaluating the capa-

bility of the same model to predict some experimentally observed results on slender structures. Vandiver et al. [20] presented a summary of a large experimental campaign, where cables were tested in linearly sheared flow conditions. Fig. 6 shows a simplified illustration of their experimental setup.

As seen in Fig. 6, the cable experiences a linearly sheared flow on part of its span. The other part is in stagnant water. They studied the effect of two parameters on the cable vibration response. The first one is the shear of the flow,  $\beta = \Delta U / U_{ref}$ , and the second one is the number of the cable vibration modes that are in the range of vortex-induced excitation. These modes are such that their frequency  $f$  falls

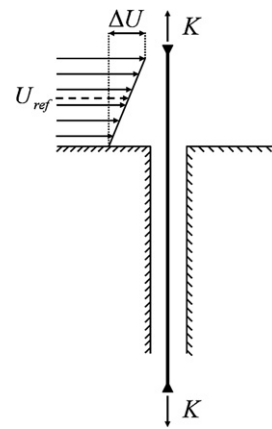


Fig. 6. Experimental configuration of tensioned cable under shear flow, Case IV [20].

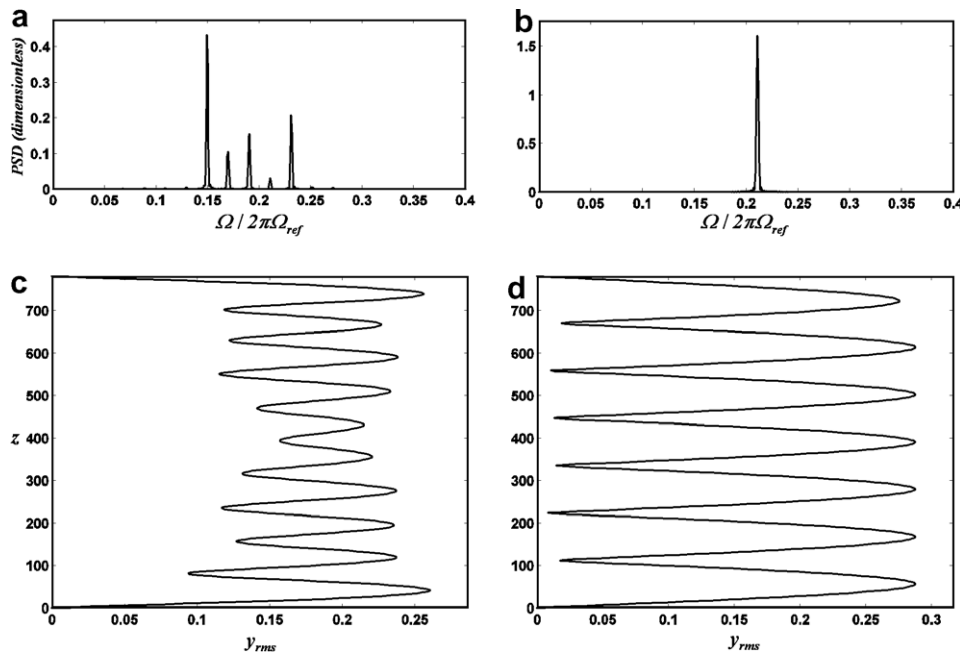


Fig. 7. Effect of the flow shear parameter  $\beta$  on the number of modes contributing to the response of the cable, Case IV. Low shear,  $\beta = 1.2$ , shows multimodal response. High shear,  $\beta = 1.8$ , shows single-mode response. (a), (b) PSD of cable displacement for  $\beta = 1.2$  and  $\beta = 1.8$  respectively; (c), (d) r.m.s. value for  $\beta = 1.2$  and  $\beta = 1.8$  respectively.

in the range of shedding frequencies corresponding to the range of flow velocity, i.e.

$$\frac{St}{D} \left( U_{\text{ref}} - \frac{\Delta U}{2} \right) < f < \frac{St}{D} \left( U_{\text{ref}} + \frac{\Delta U}{2} \right). \quad (7)$$

Vandiver et al. [20] observed multimodal cable response for low shear value, but when increasing the shear over a threshold value, while keeping the number of excited modes constant, the cable response became dominated by one mode (Fig. 3 in [20]).

The same configuration is computed with the wake oscillator model to reproduce the aforementioned experimental result. Two test cases reported here are referred to Case IV. The parameters used for both simulations appear in Table 1. The shear values  $\beta$  used for the first and second test case are 1.2 and 1.8, respectively. For both cases, the number of excited cable modes is 10, which requires to adapt the dimensionless tension  $c$  (see Table 1). As in the previous section, a random noise of order  $O(10^{-3})$  of amplitude was applied as initial condition to the fluid variable  $q$ . Cable extremities are fixed. The numerical integrations are carried out for several hundreds vibration cycles in order to achieve acceptable frequency resolution for spectral analysis. Fig. 7a and b shows the dimensionless power spectrum density (PSD) of the cable response at an arbitrary point for both numerical integrations ( $z = 680$ ). A single dominant peak appears for the integration done with the shear value of 1.8 (Fig. 7b). This means that the response is then dominated by a single frequency as the cable response is thus characterised by a single vibration mode. For the simulation done with a shear value of 1.2 (Fig. 7a), there are multiple peaks in the PSD meaning a multimode response. Fig. 7c and d shows the displacement profile along the cable span for the two cases. In Fig. 7c, several modes contribute to the response, while Fig. 7d shows a single mode response. The transition from multimode to single-mode response was found by Vandiver et al. [20] near  $\beta = 1.6$  (see Fig. 3 in [20]). From the results shown in Fig. 7, it can be concluded that the wake oscillator model reproduces in a qualitative manner the transition of the cable dynamic behavior observed experimentally by Vandiver et al. [20].

## 5. Concluding remarks

In the comparison presented above, it was shown that some of the important features of the dynamics of long cylinders undergoing VIV can be modeled using a simple wake oscillator approach. These features are essentially the standing or propagative nature of waves (Case I–III), and the modal content of the response (Case IV). These three dimensional characteristics have been recovered using only a phenomenological model based on two dimensional modelisation of VIV. No additional term has been used in the model for the wake dynamics and the coupling with the structure. Because of the simplicity of the model, all the results presented in this paper required a small computa-

tional time: typically, a few minutes to an hour of CPU on a PC. As of today, this is one of the main advantages of the phenomenological approach over the DNS computations. This would allow undertaking large parametrical studies of VIV of long systems which are needed for practical applications.

In terms of applications to cases of higher Reynolds numbers, it is only needed in this phenomenological approach to incorporate the dependence of the coefficients on Reynolds number. Most of these are known from two dimensional experimental results. In fact, this is another advantage of this approach as state of the art knowledge on wake dynamics and VIV can be incorporated in the model. Computation costs are thus independent of Reynolds number here. However, by nature, this method cannot provide refined results on the wake structure such as those obtained by DNS in [15].

In all presented cases as well as in recently published results cited in this paper, it appears that the dynamics of long slender system undergoing VIV is quite complex. To illustrate this, it was found that different initial conditions sometimes lead to distinct steady state behaviors as could be expected in a strongly non-linear autonomous system. Thus, a statistical assessment of the effect of initial conditions and even of all parameters would be useful. This is in the range of feasibility with the wake oscillator model.

An important issue is also the range of applicability of this kind of model. By nature, all empirical (or phenomenological) models make use of experimental data from simple experiments to predict more complex cases. In VIV, this is the case of most approaches, as the direct computation of the flow (DNS) is still impossible in engineering practice. Systematic validation, as presented here, and the search for a physical understanding of the elementary mechanisms that take place in VIV and VIW is of the utmost importance to assess the range of applicability. Note that the discretization errors are certainly far smaller than all uncertainties pertaining to the physical mechanisms involved.

Finally, it is hoped that some of the essential features of three dimensional dynamics of these VIV and VIW can be understood using an energy balance or even linear stability analysis with our model. This is under current investigation; see for instance [11].

## Acknowledgements

We would like to thank Matteo Facchinetti and Lionel Mathelin for fruitful discussions and Didier Lucor for making available to us results before publication.

## References

- [1] Bearman PW, Chaplin JR, Fontaine E, Graham JMR, Herfjord K, Lima A, Meneghini JR, Schulz KW, Willden RHJ. Comparison of CFD predictions of multi-mode vortex-induced vibrations of a tension riser with laboratory measurements. In: Paidoussis MP, editor. Proceedings of the 6th international symposium on FSI, AE and FIV: ASME PVP Division Summer Meeting, Vancouver; 2006.

- [2] Birkoff G, Zarantanello EH. *Jets, wakes and cavities*. New York: Academic Press; 1957.
- [3] Bishop RED, Hassan AY. The lift and the drag forces on a circular cylinder oscillating in a flowing fluid. *Proc Roy Soc London – Series A* 1964;277:51–75.
- [4] Blevins RD. *Flow-induced vibration*. New York: Van Nostrand Reinhold; 1990.
- [5] Chaplin JR, Bearman PW, Cheng Y, Fontaine E, Graham JMR, Herfjord K, et al. Blind predictions of laboratory measurements of vortex-induced vibrations of a tension riser. *J Fluids Struct* 2005;21: 25–40.
- [6] Facchinetti ML, de Langre E, Biolley F. Vortex shedding modeling using diffusive van der Pol oscillators. *C.R. Mécanique* 2002;330: 451–6.
- [7] Facchinetti ML, de Langre E, Biolley F. Coupling of structure and wake oscillators in vortex-induced vibrations. *J Fluids Struct* 2004;19: 123–40.
- [8] Facchinetti ML, de Langre E, Biolley F. Vortex-induced travelling waves along a cable. *Eur J Mech B/Fluids* 2004;23:199–208.
- [9] Gabbai RD, Benaroya H. An overview of modeling and experiments of vortex-induced vibration of circular cylinders. *J Sound Vib* 2005;282:575–616.
- [10] Hartlen RT, Currie IG. Lift-oscillator model for vortex-induced vibrations. *J Eng Mech Div EM5* 1970:577–91.
- [11] de Langre E. Frequency lock-in is caused by coupled-mode flutter. *J Fluids Struct* 2006;22:783–91.
- [12] Lucor D, Mukundan H, Triantafyllou MS. Riser modal identification in CFD and full-scale experiment. *J Fluids Struct* 2006;22:905–17.
- [13] Marcollo H, Hindwood JB. On shear flow single mode lock-in with both cross-flow and in-line mechanisms. *J Fluids Struct* 2006;22: 197–211.
- [14] Mathelin L, de Langre E. Vortex-induced vibrations and waves under shear flow with a wake oscillator model. *Eur J Mech B/Fluids* 2005;24:478–90.
- [15] Newman DJ, Karniadakis GE. A direct numerical simulation study of flow past a freely vibrating cable. *J Fluid Mech* 1997;344:95–136.
- [16] Norberg C. Fluctuating lift on a circular cylinder: review and new measurements. *J Fluids Struct* 2002;17:56–96.
- [17] Riley KF, Hobson MP, Bence SJ. *Mathematical methods for physics and engineering*. Cambridge: Cambridge university press; 1998.
- [18] Sarpkaya T. A critical review of the intrinsic nature of vortex-induced vibrations. *J Fluids Struct* 2004;19:389–447.
- [19] Vandiver JK. Dimensionless parameters important to the prediction of vortex-induced vibration of long, flexible cylinders in ocean currents. *J Fluids Struct* 1993;7:423–55.
- [20] Vandiver JK, Allen D, Li L. The occurrence of lock-in under highly sheared conditions. *J Fluids Struct* 1996;10:555–61.
- [21] Williamson CHK, Govardhan R. Vortex-induced vibrations. *Annu Rev Fluid Mech* 2004;413–55.